Available online at www.garmian.edu.krd

Passer Journal

Passer 2 (2020) 69- 75

http://passer.garmian.edu.krd/

The Influence of Various Reactants in the Growth Solution on the Morphological and Structural Properties of ZnO Nanorods

Ahmed Fattah Abdulrahman *

Department of Physics, Faculty of Science, University of Zakho, Zakho, Kurdistan Region, Iraq

Received 27 August 2020; revised 12 October 2020;
accepted 13 October 2020; available online 26 October 2020

doi:10.24271/psr.14

ABSTRACT

In the current work, the effect of three different Zinc (Zn) salts as reactants precursors in the growth solution on the characteristic properties of the Zinc oxide (ZnO) nanorods (NRs) was investigated and reported. High quality hexagonal ZnO NRs have been grown on the glass-slide substrates via the chemical-bath deposition (CBD) approach at 90 ºC. The radio-frequency sputtering (RF) technique has been used to coat the 150 nm of ZnO nano-seed layer over the whole glass-slide substrates. The Field-emission scanning electron microscopy (FESEM), the Energy-dispersive characterization (EDX), and the X-ray diffraction (XRD) characterizations have been used to characterize and examination of the morphological, chemical compositional, and structural characteristics with ZnO hexagonal-wurtzite structure of the NRs. The used zinc salts were Zinc-nitrate Hexahydrate (ZNH), Zinc-acetate (ZA), and Zinc-chloride (ZC). The FESEM and XRD results indicated that the change in types of Zinc salts with Methenamine as reactants precursors in the growth (deposition) solution have a remarkable and significant impact on the surface topography (morphology) characteristics and structural characteristics of synthesized ZnO NRs. The average size and average length of the grown ZnO NRs were in the range of (91-529) nm and (1008-3189) nm, respectively. The high aspect ratio was obtained of ZnO NRs synthesized from Zinc-nitrate Hexahydrate salt and was about 11. The highest growth rate was investigated ZnO NRs synthesized from Zinc-chloride salt and was about 17.716 nm/min. The average crystalline size of synthesized ZnO nanorods was in the range (48.35-56.06) nm.

Keywords: Growth Solution, ZnO Nanorods, Zinc Salts, Methenamine, CBD

1. Introduction

ZnO is the n-type semiconductor that has considerable electronic and photonic materials with a wide direct optical energy band-gap (3.37 eV), extensive exciton binding-energy (60 meV at room-temperature (RT)), greater thermal and chemical constancy, biocompatibility translucence and a massive area of electrical accessibility [1-3]. These excellent properties make ZnO a promising semiconductor material in excitonic emissions and lasing applications over the room-temperature compared with other materials. In addition, due to its excellent chemicals and thermal properties, the ZnO also has piezoelectric and photo-conducting characteristics. Thus, it has the opportunity in a broad very of implementations, such as for biomedical uses, ultraviolet (UV) optical nano-devices, gas sensing, light-emitting diode, and photovoltaic cells, [4-10]. ZnO can be fabricated in several types of nanostructures form such as nanorods, nanowires, nanoparticles, nanodisks, nanoflowers, nanosheets, nanofibers, and others [11-14]. These different ZnO nanostructures have been synthesized on the wide domain of substrates by using various physical, and chemical techniques [15].

The techniques comprise metallic-organic chemical-vapor deposition method (MOCVD) [16], pulsed-laser deposition (PLD) method [17], chemical-vapor deposition method [18], radio-frequency magnetron (RF) sputtering technique [19], electrochemical-deposition (ECD) method [20], sol-gel method, vapor-phase transport (VPT) method [21], spray pyrolysis techniques, and chemical bath deposition (CBD) [22]. During these techniques, the CBD is more flexible approach to synthesis ZnO nanostructures with powerful control on their morphology due to its benefits [23]. These benefits are low temperature (<100 ºC), very simple method, non-costly, non-dangerous technique, obtainability of beginning chemical substance, manufacturing of high-density arrays, large growth ability, utilize of environment-pleasant chemical materials, and doesn't require using the intricate growth system [24]. The surface morphology (density distribution, shape, length, and size), alignment, orientation, and structure of ZnO NRs manufactured via the CBD method can be

* Corresponding author
E-mail address: ahmed.abdulrahman@uoz.edu.krd (Instructor).
Peer-reviewed under the responsibility of the University of Garmian.

controlled effectively by adjusting the main different synthesis parameters (conditions) like synthesis duration (time), pH value of synthesis chemical solution, the molar ratio of precursor concentration of the reactants, synthesis temperature, annealing duration, and annealing temperature [24]. Further, the different reactants (Zinc Salt) in the growth solution are another significant growth and preparation parameter that have an important influence on the orientation, surface-topography, structure, and quality of ZnO NRs.

In literature, there are just a small number of researchers who are interested in the current topic. The most researchers are focused on one type of Zinc salt with Methenamine as the reactant in the growth solution for growing ZnO nanorods. To the best of my information and knowledge, it is the first time to investigate the effect of three various zinc salt with Methenamine as a reactant in the growth solution on the growth of ZnO NRs. In this work, the study and the investigation for the effect of the three different zinc salts (ZNH, ZA, ZC) as a reactant precursor in the growth solution on the surface topography (top and side views), aspect ratio, growth rate, alignment, orientation, shape, density distribution, size, and structural properties of ZnO nanorods have been achieved. Also, the optimum zinc salt as the effective reactant's precursor in the growth solution of ZnO NRs growth has been obtained and reported.

2. Experimental Details

Each chemical material was bought from Sigma-Aldrich (SA) Company. The ZNH ($Zn(NO_3)_2.6H_2O$), ZA ($Zn(O_2CCH_3)_2(H_2O)_2$), ZC ($ZnCl_2$), and Methenamine ($C_6H_{12}N_4$) have been utilized as the beginning chemical materials without moreover purification with a purity range of 99%.

2. 1 ZnO Seed-Layer Preparation

The soda-lime microscopic-glass (MG) slide has been selected as the substrates and has been immaculate by employing an ultrasonic-bath (UB) device via ethanol (C_2H_5OH), acetone (C_3H_6O), and deionized (DI) water for 20 min, respectively, then dried by using nitrogen gas (N_2) [25]. The RF sputtering has been employed by utilizing target of ZnO with a purity range of 99.999% to coat about 150 nm of zinc oxide seed-layer on the cleaned soda-lime microscopic glass slide substrates. This process achieved under a pressure of the Argon gas (Ar) of 5.8 $*10^{-6}$ Pascal and the power of RF magnetron sputtering of 0.18 watt for 20 min. After completing the formation of the ZnO seed-layer on glass slide substrates, the prepared samples have been inserted carefully in the annealing-tube furnace at the temperature of 573.15 K for 120 min to make better structural fineness and optical characteristics of the zinc oxide seed-layer coated glass substrates [26, 27].

2. 2 CBD Growth Process

The ZnO NRs were fabricated via a low-cost CBD approach for different reactants in the growth solution. The ZNH, ZA, ZC, and Methenamine have been applied as the precursors of reactants in the growth (deposition) solution and the DI-water was used as the solvent. The 0.1 Mol of each ZNH and Methenamine 1:1 was separately dissolved in DI water and both were mixed with each other by utilizing a magnetic stirrer and the corresponding sample was labeled as **(a)**. The equal molar concentration (0.1 Mol) of each ZA and ($C_6H_{12}N_4$) was one by one thawed in DI-water, then both blended under a magnetic stirrer machine and the created sample was classified as **(b)**. The 0.1 Mol of each ZC and ($C_6H_{12}N_4$) has been once one by one thawed in DI-water and both blended via a magnetic stirrer device and the result classified as sample **(c)** [26]. To investigate the influence of the several Zinc Salts with Methenamine as the various reactants in the growth solution on the topography, density distribution, diameter, length, alignment, orientation, form, and crystal structure of the Zinc oxide NRs, the prepared annealed ZnO SL deposited glass-slide substrates have been one by one carefully inserted vertically into a three-beaker comprising of the admixture of the two synthesis chemical solutions for three samples. The three beakers have been converted carefully inside a laboratory oven at 90 °C for 180 min. After completion of the CBD process of ZnO NRs, the fabricated zinc oxide NRs samples were first brought out of the growth (deposition) solution with swilled and washed via DI-water to drive out the residual salt, and subsequently it was desiccated with nitrogen gas [26].

2. 3 Characterization Techniques

The surface morphology, orientation, form (shape), distribution, diameter (size), homogeneously, alignment, length (height), and elemental composition of synthesized ZnO NRs have been characterized and examined by using the FESEM (Carl-Zeiss, 50-VP (Leo-Supra), and FEI Nova (nanosem-450)) technique and Energy-Dispersive X-Ray (EDX) analysis, respectively. The crystal structure and size, the epitaxial growth goodness (quality), the stress, and the strain, of Zinc oxide NRs on glass-slide substrates have been characterized and examined by utilizing the system of high-resolution XRD (HR-XRD) with model Pro MRD, X-Pert. The wavelength (λ) of CuK α radiation (1.54050 Angstrom) with (2θ) of the scanning range (20° – 80°).

3. Results and Discussion

3. 1 *FESEM Analysis*

The surface topography (top and side views), the orientation, the size (diameter), the homogeneity the length, the alignment, and the density distribution of ZnO NRs have been studies by utilizing FESEM measurements. Figure 1 displays the top and side (cross-section) views of very well-aligned ZnO NRs synthesized from different zinc salt with Methenamine as a reactant in the growth solutions. The investigated FESEM figures showed the produced zinc oxide NRs was vertically fully aligned with a hexagonal shape and had the high-density distribution upon the whole surface of the glass-slide substrates. Figures 1 (a and d) demonstrates that the synthesized ZnO NRs from ZNH with Methenamine. It was noted that the most ZnO NRs were grown vertically well-aligned and oriented structure and have homogenous density upon the whole substrate with an average diameter of 91 nm and the average length of 1008 nm. The average diameter and length of grown ZnO NRs from ZA with Methenamine were increments to 331 nm and 2102 nm, respectively as demonstrated in Figure (1b). It noted that the fabricated NRs were perpendicularly oriented with high distribution density of NRs or microrods and have a hexagonal shape with non-uniform size, non-uniform high and the most produced ZnO NRs were grown like a group. Figure 1 (c) shows

the high distribution density and perfect hexagonal shape of ZnO NRs synthesized from ZC with Methenamine. It can be observed that the ZnO NRs were uniform oriented and most obtained ZnO nanorods or micro-rods growth group shape or set of rods with an average size of 529 nm and the average length was 3189 nm. The various reactants (zinc salts) in the growth solution was the remarkable and significant parameter (condition) to control each of the topography (morphology), the diameter, the alignment, the form, the distribution density, the orientation, and the thickness of the ZnO NRs.

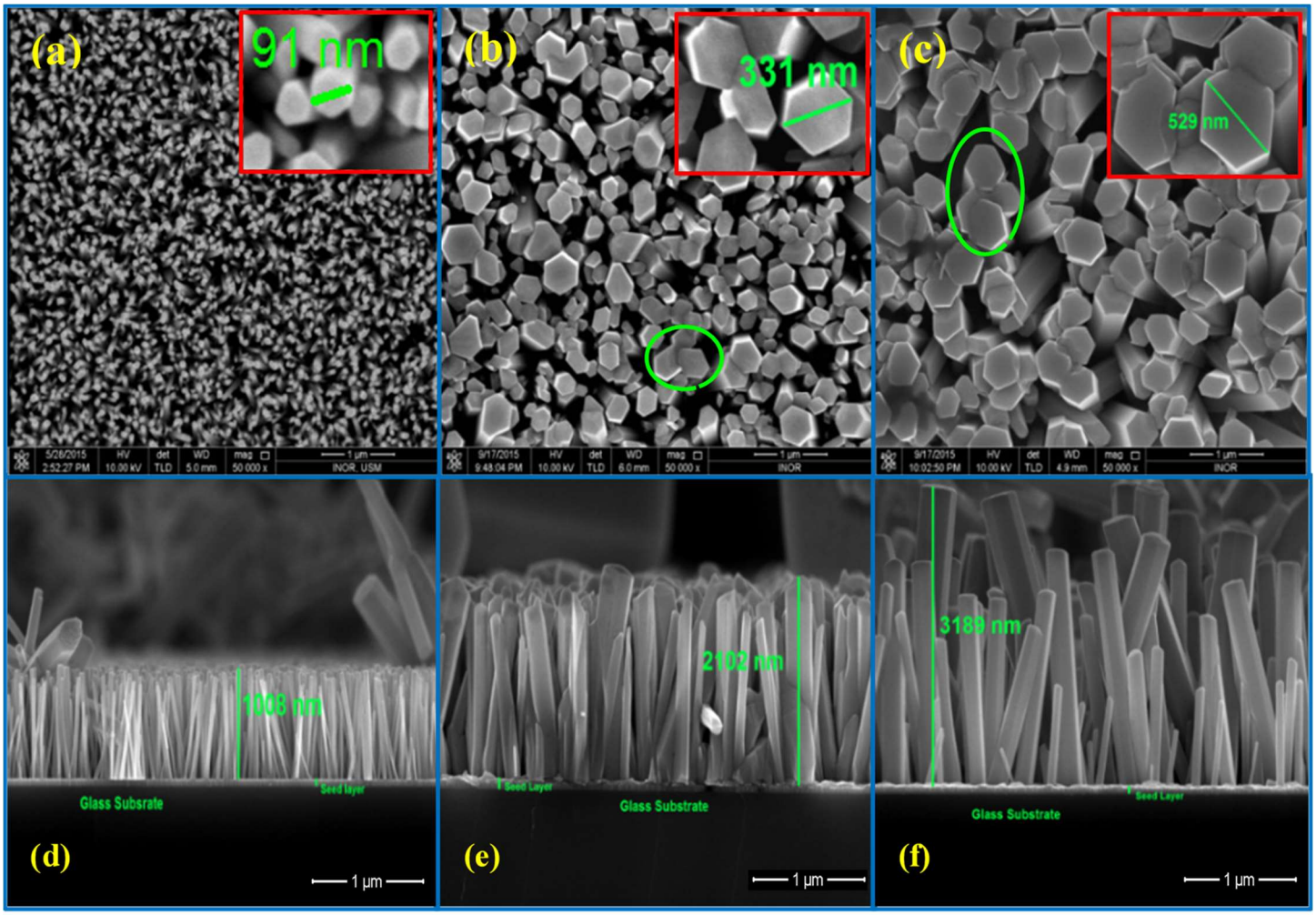

Figure 1: Top and Side Views FESEM Images of ZnO NRs synthesized from Various Reactants in the Growth-Solution

More characterizations of the different zinc salts as a reactants precursor in the growth solution effect on the average size (diameter), the average height (length), the aspect-ratio which is defined the length per unit diameter, and the growth rate of the NRs with Initial pH, and final pH were listed in Table 1.

Table 1: Summarized Data Calculated from FESEM of ZnO NRs synthesized from Different Reactants in the Growth Solution

Growth Solution	Initial pH	Final pH	Average Size (nm)	Average Length (nm)	Aspect Ratio	Growth Rate (nm/min)
ZNH	6.7	5.8	91	1008	11.077	5.600
ZA	7.2	6.3	331	2102	6.3500	11.677
ZC	6.6	5.5	529	3189	6.0254	17.716

It has appeared that the variation in the values of the aspect-ratio of the NRs formed from three several zinc salts. Besides, the estimated values of the aspect-ratio of ZnO NRs were about 11, 6.35, and 6 for ZNH, ZA, and ZC, respectively. This exitance variation in values of the aspect-ratio is possibly due to the average size and it is smaller than the average length of the NRs formed from ZNH compared to the other zinc salts and were about 91 nm and 1008 nm, respectively. It can presume also that

the optimum zinc salt as a reactant precursor in the growth solution was ZNH with Methenamine because the synthesized ZnO NRs have a high value of the aspect-ratio above to 11 confronted with the other zinc salts as a reactant in the growth solution. The growth rate of the synthesized NRs from different reactants in the growth solution (length per unit CBD growth time) were listed in Table 1. It can observe that the growth rate was reduced at 180 min, and the growth rate of the NRs grown form ZNH, ZA, and ZC were 5.60 nm/min, 11.677 nm/min, and 17.716 nm/min, respectively. The maximum growth rate is obtained of ZnO nanorods grown with ZC; This is due to the ZnO nanorods grown at ZC, which they are longer than the ZnO nanorods grown from other zinc salts. The initial and the final pH values of the different zinc salts as reactants precursor in the growth solution were very carefully reading prior and after the CBD deposition process and were summarized in Table 1. It was observed that the values of the final pH (after CBD growth finish) of the growth solution was decreased compared to the initial pH. This decrease means that there is a lower existence of (OH) ions in the growth solution, which resort to merging readily with the Zinc. Further, the high growth rates do not conserve the sufficient Zn in the solution in the shape (form) of the Zn $(OH)_2$ [28].

3.2 Energy-Dispersive X-Ray (EDX) Analysis

The elementals chemical structures of the formed zinc oxide NRs from various reactants in the growth solutions were investigated by using EDS (EDX) characterizations. Figure 2 exposes the identifying EDX characterizations, which discloses the subsistence of the zinc (Zn) and the Oxygen (O), which identity to the structures properties of the ZnO, without the existence of any defects or substrate signal according to limitations of the EDS. The atomic ratio among the Zn and the O has been almost the same ratio for all characterized ZnO NRs samples formed from several reactants (zinc salts) in the growth solution on glass-slide substrates. The molecular-ratio (MR) of the Zinc: Oxygen of the fabricated NRs estimated from quantitative EDS (EDX) characterizations data was nearly 1:1, which is proving the grown NRs were pure zinc oxide.

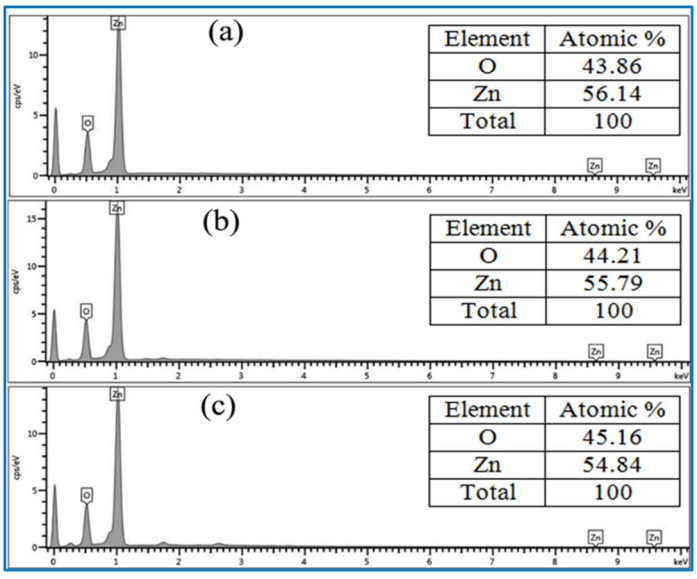

Figure 2: Typical EDX Characterization of the ZnO NRs synthesized from Various Reactants in the Growth Solution

3. 3 X-Ray Diffraction (XRD) Characterization

The XRD patterns of ZnO NRs grown for different reactants (zinc salts) in the growth solution at 90 °C have appeared in Figure 3. All the peaks of diffraction in whole XRD patterns were listed as the ZnO wurtzite hexagonal phase, which was corresponded to the standard database spectrum (01-080-0074 Number of the JCPDS cards). Besides, there are no peaks of diffraction have been demonstrated from other impurities, proving the high purity of the zinc oxide nanocrystal phase has been implemented. For all investigated and characterized zinc oxide NRs, the diffraction peak was investigated at 2θ = 34.4, which is corresponding to the zinc oxide (002) plane, finding the oriented preferentially growth alongside the (002) c-axis. The nanorods resorted to formed in the orientation alongside (002) plane. The free surface-energy density of this orientation was lowest in the zinc oxide crystal [29]. The acute and strong of the ZnO alongside (002) peak diffraction in all patterns of the XRD, also assured that the Zinc oxide NRs were formed preferentially alongside the c-axis of the ZnO wurtzite hexagonal structure with very weak diffractions peaks from other surfaces, which is confirmed that the ZnO NRs were vertically well-aligned grow on the whole surface of glass slide substrates.

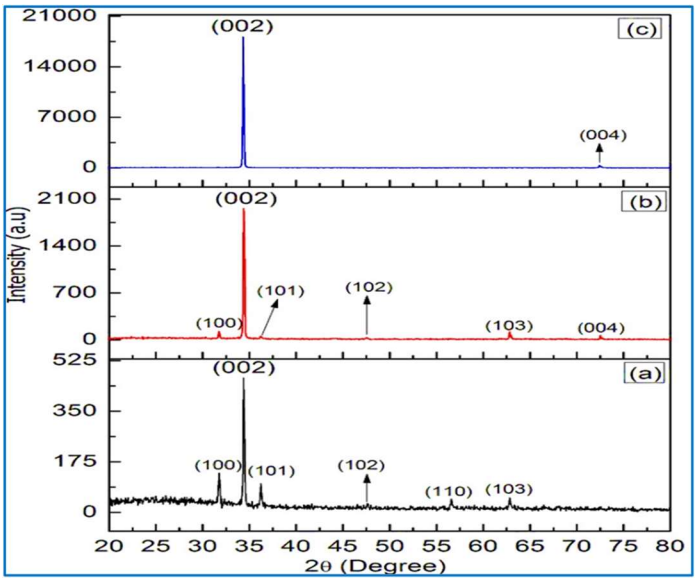

Figure 3: The XRD of the ZnO NRs synthesized from Various Reactants in the Growth Solution

Figure (3a) reveals the X-ray diffraction pattern of the ZnO NRs, which created from ZNH with Methenamine. It was obtained that the strong peak along (002) plane at the value of 2θ (34.425) and other surfaces showed the low intensity of the diffraction peaks. This affirms the enhancement alignment of the most zinc oxide NRs formed well-vertically over the whole glass-slide substrate. The XRD pattern of fabricated ZnO NRs from ZA with Methenamine was displayed in Figure (3b). It can seem that the strong diffraction peak in the direction of the c-axis (002) at a 2θ value of (34.375). Besides, the XRD pattern of synthesized ZnO NRs from ZC with Methenamine was revealed in Figure (3c). It can note the strong diffraction peak of the ZnO was in a direction along the c-axis (002) at the 2θ value of (34.325). This gives all NRs grow vertically well-aligned over the entire glass substrate.

Figure 3 and Table 2 shows that the peak diffraction intensity alongside (002) plane was raised of the NRs produced from different reactants in the growth solutions and were 465, 1958, and 18114 for ZNH, ZA, and ZC, respectively. From XRD results, it is observed that ZnO diffraction peaks alongside (002) became narrower and higher as ZnO NRs fabricated from the growth solution of ZC and Methenamine. It was also found that ZnO crystalline quality became better ZnO NRs were grown from the other two growth solutions. The lattice parameters (constants) (a and c) of the ZnO wurtzite hexagonal structure alongside diffraction peak (002) plane were estimated using Bragg's law [30], as shown in Table 2.

$$a = \sqrt{\frac{1}{3}}\frac{\lambda}{\sin\theta} \quad (1)$$

$$c = \frac{\lambda}{\sin\theta} \quad (2)$$

Where λ is the X-ray source wavelength and (θ) is the diffraction peak angle.

Table 2: Lattice constants (Parameters) and zinc oxide wurtzite-hexagonal Structure Characteristics of the Nanorods alongside Peak Diffraction (002) plane synthesized from Different Reactants in the Growth Solution

Growth Solution	2θ	FWHM	I (a. u)	a (Å)	c (Å)	$\mathfrak{E}_a$%	$\mathfrak{E}_c$%	d (Å)
ZNH	34.425	0.172	465	3.0058	5.206	-7.65	-0.069	2.603
ZA	34.375	0.161	1958	3.0100	5.213	-7.48	-0.029	2.607
ZC	34.325	0.148	18114	3.0143	5.220	-7.35	0.111	2.610

The tensile and compressive strains ($\mathfrak{E}_c$) and ($\mathfrak{E}_a$) of the NRs produced on the whole glass slide substrate alongside (a and c) axis, respectively and have been evaluated by using the following equations [31, 32]:

$$\mathfrak{E}_a = \frac{a-a_o}{a_o} \times 100\% \quad (3)$$

$$\mathfrak{E}_c = \frac{c-c_o}{c_o} \times 100\% \quad (4)$$

Where (a_o =3.2535 & c_o =5.2151) were illustrated the criterions lattice parameters (constants) for unstrained (bulk) zinc oxide NRs and nanostructures, which was existence in the mentioned database (01-080-0074 JCPDS cards).

The strain alongside c-axis for ZnO samples a-c were -0.069%, -0.029% and 0.111%, respectively. The strains also alongside a-axis for ZnO samples a-c were -7.62%, -7.48%, and -7.35% respectively. The appearance positive-value of strain was concerned with the tensile-strain and explores an expansion in the lattice parameter (constant), but the appearance negative-value of strain was related to the compressive-strain and explores the contraction of the lattice. The plane-spacing (distance) of the ZnO wurtzite-hexagonal structure of the NRs alongside (002) plane was evaluated from to the Bragg's law [33], and it is listed in Table 2. It was observed that the plane spacing increased from the sample (a-c) along the c-axis (002). This is due to the diffraction peak intensity was sharply increased and FWHM and 2θ were decreased.

$$\frac{1}{d^2} = \frac{4}{3}\left(\frac{h^2+hk+k^2}{a^2}\right) + \frac{l^2}{c^2} \quad (5)$$

Where (*a* & *c)* were defined the lattice parameters (constants). The average crystal size (particle size) of the zinc oxide NRs for peak diffraction on (002) plane has been determined via formula of the Debye-Scherer [34, 35] and it were listed in the Table 3.

$$D = \frac{k\lambda}{\beta\cos\theta} \quad (6)$$

Where (k) has been defined the constant, which was elected to be (0.9), the (λ) is the X-ray source wavelength, the (β) is full-width at half-maximum (FWHM) in radian, and the (θ) is the angle Bragg diffraction.

Table 3: Crystal size, Dislocation Density, Volume and Bond Length of ZnO NRs alongside (002) Peak Diffraction Grown for Different Reactants in the Growth Solution

Growth Solution	D (nm)	δ*10^{-6} (Å^{-2})	V (Å^3)	L (Å)
ZNH	48.35	4.277	40.74	1.880
ZA	51.72	3.738	40.91	1.883
ZC	56.06	3.183	41.08	1.886

The obtained crystals sizes of ZnO NRs were increased by 48.35 nm, 51.72 nm, and 56.06 nm for ZNH, ZA, and ZC, respectively, due to the decreases in FWHM values of ZnO diffraction peak alongside (002). The number of defects (impurities) in the ZnO crystal, which was called the dislocation density (δ) has been evaluated via the following equation [36] and is listed in Table 3.

$$\delta = \frac{1}{D^2} \quad (7)$$

Where D is crystallite size.

As shown in Table 3, the number of impurities is decreased when ZnO NRs were fabricated from the growth solution from ZNH to ZC. This decrease in the values of dislocation density is due to the variation in the crystal size, high crystal quality, and (sharp, high, strong, and narrow of diffraction peak alongside (002)) of ZnO NRs grown from ZC salt.

The zinc oxide NRs hexagonal cell volume and ZnO NRs bond length have been calculated using the below equations (8 – 9) [37] and were listed and summarized in Table 3.

$$L = \sqrt{\frac{a^2}{3} + \left(\frac{1}{2} - u\right)^2 c^2} \quad (8)$$

Where (u) is the positional parameter (condition) in the ZnO wurtzite-hexagonal structure, which was regarded to the ratio of (c/a). The (u) was estimated (measured) of the amount by, which each atom was displaced relating the next alongside the (c-axis) and which was state by following formula [37]:

$$u = \frac{a^2}{3c^2} + 0.25 \quad (9)$$

The ZnO NRs hexagonal cell volume (V) has been investigated via the below equation [37]:

$$V = \frac{\sqrt{3}}{2} a^2 c \quad (10)$$

From the Table 3, it is to be noted that both hexagonal cell volume and bond length of synthesized NRs were increased in the range of (40.74 - 41.08) $Å^3$ and (1.880 -1886) Å, respectively. This increase is caused by the decreases in the value of peak position (2θ) of ZnO peak diffraction alongside (002). Both also were directly dependent on the lattice constants (a & c) which are dependent on the value of peak position (2θ).

4. Conclusion

The vertical well-aligned along c-axis (002) and high crystalline of the ZnO NRs have been successfully fabricated via the very simple CBD method for various zinc salts. It was found that the various zinc salts as reactant precursor in the growth solution have a significant impact on the morphological properties, aspect ratio, growth rate, size, structural properties of the produced ZnO NRs. The FESEM and the XRD results were explained that the NRs with wurtzite hexagonal ZnO structure have been grown vertically well-aligned and densely over the whole glass slide substrates. From the results, it is noted that the optimum zinc salt as reactant in the growth solution was Zinc nitrate Hexahydrate (ZNH) with Methenamine. This is caused by the synthesized ZnO NRs from the zinc salt, which has high aspect ratio, uniform orientation, the same length, and high densely distribution, uniform diameters and nanorods or nanowires. This technique has a beneficial application for nano-optoelectronic devices efficiency such as LED, UV detector, and solar cells, they improved the quality and responsivity of devices.

References

1. Morkoc, H. Ozgur, U., General Properties of ZnO, in Zinc Oxide: Fundamentals, materials and device technology, *Wiley-VCH Verlag GmbH & Co. KGaA*, 1-76, (2009).
2. P. Suresh Kumar, M. Yogeshwari, A. Dhayal Raj, D. Mangalaraj, D. Nataraj1, and U. Pal, Synthesis of Vertical ZnO Nanorods on Glass Substrates by Simple Chemical Method, *Journal of Nano Research* **5**, 223-230, (2009).
3. Ahmed F. Abdulrahman, Sabah M. Ahmed, Naser M. Ahmed & Munirah A. Almessiere, Different Substrates Effects on the topography and the structure of The ZnO Nanorods Grown By Chemical Bath Deposition Method, *Digest Journal of Nanomaterials and Biostructures* **11***(3)*, 1007, (2016).
4. Kyung Ho Kim, Kazuomi Utashiro, Yoshio Abe, and Midori Kawamura, Growth of Zinc Oxide Nanorods Using Various Seed Layer Annealing Temperatures and Substrate Materials, Int. J. Electrochem. Sci. **9**, (2014).
5. S.S. Shinde, K.Y. Rajpure, High-performance UV detector based on Ga-doped zinc oxide thin films, *Appl. Surf. Sci.* **257**, 9595–9599, (2011).
6. Y. R. Ryu, T. S. Lee, J. A. Lubguban, H. W. White, B. J. Kim, Y. S. Park, and C. J. Youn, Next generation of oxide photonic devices: ZnO-based ultraviolet light-emitting diodes, *Appl. Phys. Lett.* **88** (24), 241108, (2006).
7. A.I. Hochbaum, P. Yang, Semiconductor nanowires for energy conversion", *Chem. Rev.,* **110,** 527, (2010).
8. Hey-Jin L., Deuk Y. L. and Young O., Gas sensing properties of ZnO thin films prepared by microcontact printing, *Sensors and Actuators A: Physical*, **125** (2), 405-410, (2006).
9. Marte R, Schmidt T, Shea H R, et al., Single- and multi-wall carbon nanotube field-effect transistors. *Appl. Phys. Lett.* **73** (17):2447-2449 (1998).
10. Abdulrahman, A.F. The effect of different substrate-inclined angles on the characteristic properties of ZnO nanorods for UV photodetectors applications. *J Mater Sci: Mater Electron* **31**, 14357–14374, (2020). https://doi.org/10.1007/s10854-020-03995-3
11. M.H. Huang, S. Mao, H. Feick, H.G. Yan, Y.Y. Wu, H. Kind, E. Weber, R. Russo, P.D. Yang, Room-Temperature Ultraviolet Nanowire Nanolasers, *Science* **292**, 1897, (2001).
12. W.I. Park, D.H. Kim, S.W. Jung and G.C. Yi, Metal-organic vapor-phase epitaxial growth of vertically well-aligned ZnO NRs, *Appl. Phys. Lett.* **80**, 4232, (2002).
13. Suh H W, Kim G Y, Jung YS, Choi WK, Byun D, Growth and properties of ZnO nanoblade and nanoflower prepared by ultrasonic pyrolysis, *J. of Applied Physics* **97**(4), 044305, (2005).
14. G. Yi, C. Wang and W.I. Park, ZnO nanorods: synthesis, characterization and applications, *Semicond. Sci. Technol.* **20**, S22, (2005).
15. Huang, T. H., C., Mitch, M.C., UWE, J., Formation mechanism of (0001) ZnO epitaxial layer on γ-LiAlO2 (100) substrate by chemical vapor deposition semiconductor devices, materials & processing, *J. Electrochem. Soc.***158**, 38, (2011).
16. D. Montenegro, V. Hortelano, O. Martinez, M. Martínez Tomas, V. Sallet,V. Muñoz-Sanjosé, J. Jiménez, Influence of metal organic chemical vapor deposition growth conditions on vibrational and luminescent properties of ZnO nanorods, *J. Appl. Phys.***113**, 143513–143519, (2013).
17. J.H. Choi, H. Tabata, T. Kawai, *J. Cryst. Growth* **226**,493, (2001).
18. P. Yang, H. Yan, S. Mao, R. Russo, J. Johnson, R. Saykally, N. Morris, J. Pham, R. He, H.-J. Choi, Controlled Growth of ZnO nanowires and their optical properties, *Adv. Funct. Mater.***12**,323, (2002).
19. J.Y. Lee, Y.S. Choi, J.H. Kim, M.O. Park, S. Im, Optimizing n ZnO/PSi heterojunctions for photodiode applications, *Thin Solid Films* **403**,553, (2002).
20. Guo HH, Zhou J Z, Lin Z H., ZnO nanorod light-emitting diodes fabricated by electrochemical approaches, *Electrochem. Commun.* **10** (1),146-150, (2008).
21. Xu, C. X.; Sun, X. W.; Dong, Z. L.; Yu, M. B., Zinc oxide nanodisks, *Appl. Phys. Lett.* **85**, 3878–3880, (2004).
22. M.G. Ambia, M.N. Islam, M.O. Hakim, The effect of deposition variables on the spray pyrolysis of ZnO thin film, *J. Mater. Sci.* **29**, 6575-6580, (1994).
23. A. F. Abdulrahman, S. M. Ahmed, N.M. Ahmed and M. A. Almessiere, "Novel Process Using Oxygen and Air Bubbling in Chemical Bath Deposition Method for Vertically Well Aligned Arrays of ZnO Nanorods, *Digest Journal of Nanomaterials and Biostructures* **11** (4), 1073-1082, (2016).
24. A. F. Abdulrahman, S. M. Ahmed, N.M. Ahmed, and M. A. Almessiere, Enhancement of ZnO Nanorods Properties using Modified Chemical Bath Deposition Method: Effect of Precursor Concentration, *Crystals* **10**, 386, (2020). doi:10.3390/cryst10050386.
25. A.F. Abdulrahman, S. M. Ahmed and N. M. Ahmed, The Influence of the Growth Time on the Size and Alignment of ZnO Nanorods, *Science Journal of UOZ* **5**(1), 128-135, (2017).
26. A. F. Abdulrahman, Study the Optical Properties of The Various Deposition Solutions of ZnO Nanorods Grown on Glass Substrate Using Chemical Bath Deposition Technique, *Journal of Ovonic Research* **16**(3), 181–188, (2020).

27. A. F. Abdulrahman, S. M. Ahmed, N. .M Ahmed and M. A. Almessiere, Fabrication, characterization of ZnO nanorods on the flexible substrate (Kapton tape) via chemical bath deposition for UV photodetector applications, *AIP Conference Proceedings* 1875(1), 020004, (2017).
28. G. Amin, M.H. Asif, A. Zainelabdin, S. Zaman, O. Nur, M. Willander, Influence of pH, precursor concentration, growth time, and temperature on the morphology of ZnO nanostructures were grown by the hydrothermal method, **J. Nanomater**. (2011).
29. A. F. Abdulrahman, S. M. Ahmed and M. A. Almessiere, Effect of the Growth Time on the Optical Properties of ZnO Nanorods Grown By Low-Temperature Method, *Digest Journal of Nanomaterials and Biostructures* **12**(4),1001-1009, (2017).
30. J. Kühnle, R.B. Bergmann, J.H. Werner, Role of critical size of nuclei for liquid-phase epitaxy on polycrystalline Si films, *J. Cryst. Growth* **173**,62–68, (1997).
31. A. F. Abdulrahman, S. M. Ahmed, and N. M. Ahmed, Investigation of Optical Properties of ZnO Nanorods Grown on Different Substrates, *Science Journal of UOZ* **6**(4),160 –165, (2018).
32. D. Vernardou, G. Kenanakis, S. Couris, E. Koudoumas, E. Kymakis, N. Katsarakis, pH effect on the morphology of ZnO nanostructures grown with aqueous chemical growth, *Thin Solid Films* **515** 8764–8767, (2007).
33. M. Kashif, U. Hashim, M.E. Ali, S.M. Usman Ali, M. Rusop, Z.H. Ibupoto, M. Willander, Effect of different seed solutions on the morphology and electro-optical properties of ZnO Nanorods, *J. Nanomater*. (2012).
34. B.D. Cullity, Elements of diffraction, *Addison-Wesley publishing-companyinc*., (1978).
35. A. K. Qasim, L. A. Jamil, and A. F. Abdulrahman, Synthesis of Rutile-Tio2 Nanorod Arrays for Efficient Solar Water Splitting Via Microwave-Assisted Hydrothermal Method, *Digest Journal of Nanomaterials and Biostructures* **15**(1), 157 - 165, (2020).
36. A.H. Kurda, Y.M. Hassan, N.M. Ahmed, Controlling Diameter, Length, and Characterization of ZnO Nanorods by Simple Hydrothermal Method for Solar Cells, *World J. Nano Sci. Eng*. **5**, 34–40 (2015).
37. M. Gusatti, C.E.M. Campos, D.A.R. Souza, V.M. Moser, N.C. Kuhnen, H.G. Riella, Effect of reaction parameters on the formation and properties of ZnO nanocrystals synthesized via rapid sonochemical processing, *J. Nanosci. Nanotechnol.* **13**, 8307–8314, (2013).